

A NOVEL METHOD FOR MEASUREMENT OF ELECTRIC FIELD IN EMULATED HUMAN BODY TISSUE USING WIRE MESH SENSOR

Anis Nismayanti^{a,b*}, Marlin R. Baidillah^d, Mahfudz Al Hudad^d, Bambang Prihandoko^e, Triwikantoro^b, Endarko^b, Warsito P. Taruno^{c,d}

^aPhysics Department, University of Tadulako, Palu 94118, Central Sulawesi, Indonesia

^bPhysics Department, Institut Teknologi Sepuluh Nopember, Kampus ITS Sukolilo – Surabaya 60111, East Java, Indonesia

^cPhysics Department, University of Indonesia, Depok 16424, Indonesia

^dCenter for Medical Physics and Cancer Research Ctech Labs Edwar Technology, Tangerang 15325, Indonesia

^eResearch Center for Physics, Indonesian Institute of Science, South Tangerang 15314, Indonesia

Article history

Received

6 July 2018

Received in revised form

25 May 2019

Accepted

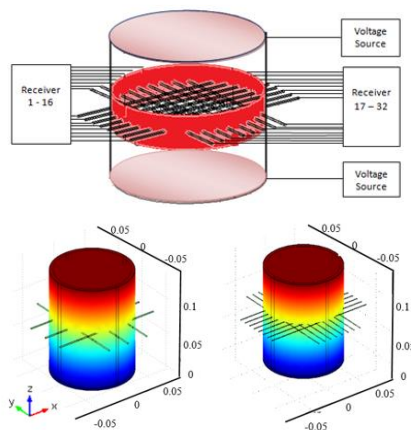
30 May 2019

Published online

26 August 2019

*Corresponding author
anis@untad.ac.id

Graphical abstract



Abstract

Wire mesh sensor has been successfully fabricated and used for measurement of the electric field in emulated human body tissue. Measurement of electric field in human body tissue needs to be done, because the electric field is very useful for the treatment especially cancer treatment and also important for health. In this study, we propose a novel electric field measurement method by using wire mesh sensor (wms), that is all channels on the wire act as receivers, and each cross point of the wire are interconnected. While in existing wire mesh sensors, there are two perpendicular channels of transmitter and receiver, and each channel is unrelated, there is a distance between the two channels. At present, wire mesh sensors 3×3 and 8×8 were used to measure the value of electric field at each wire intersection point. The wire mesh sensor consists of copper wire in a cylindrical body model with diameter 14 [cm]. The emulated human body tissue were inserted in the wire mesh sensor. Furthermore, linear back propagation technique and bilinear interpolation used for image reconstruction of the electric field distribution. The result showed that the wire mesh sensor 8×8 has better resolution than wire mesh sensor 3×3 . The characterisation of wire mesh sensor 8×8 for measurement of electric field in emulated human body tissue is obtained lower than measurement in the air with a ratio of 82%. Meanwhile, the wire mesh sensor 3×3 could be achieved at 61.8%. This study can be a new science in measuring electric field so that electric field-based treatment planning system can be more optimal.

Keywords: Electric field, emulated human body tissue, wire mesh sensor, image reconstruction, bilinear interpolation

© 2019 Penerbit UTM Press. All rights reserved

1.0 INTRODUCTION

The alternating electric field is important for medicine and health because of the alternating electric field can treat brain cancer, breast cancer, lung cancer, and skin cancer [1, 2, 3, 4].

The effect of alternating electric field on low intensity (E) 2 V/cm and intermediate frequency (f) 100 – 300 kHz can inhibit the growth of malignant tumour. The current study was tested on animal tumours, and patients with brain cancer cells, breast and lung with *in vitro* and *in vivo* methods [1], [2]. Skin cancer therapy can be performed using a pulsed alternating electric field higher than 20 kV/cm with a repetition time (T) of 30 ns over a duration of 300 ns. The result that melanoma skin cancer shrank 90% within two weeks [3]. At nanoseconds of pulse alternating electric field (nsPEF) causes the death of glioblastoma brain cancer cells in the presence of microtubule damage. The frequency of repetition used is 10 Hz at 10 ns pulse [4].

Electro-capacitive cancer therapy (ECCT) is one of the alternative for cancer treatment with low energy alternating electric field [5], [6]. The effect of anti-proliferative ECCT on tumor cells in cell and animal models was successfully investigated and the tumor was significantly reduced [7].

Determining the intensity of electric field distribution in 3D biomaterial phantom by using the numerical simulation [8]. Electrical signal characterisation of electric field measurements on human tissue has been performed using millimetre waves by Topfer [9]. The result of electrical signal characterization by simulation is that the electric field in healthy teeth and broken teeth, have different. Amplitude in the normal tooth is higher than the amplitude of the damaged tooth [9]. During this time, research related to the optimization of low energy electric field for cancer therapy is only based on simulation. All conditions in the simulation are considered ideal, but in reality not so. So it takes experiments to get clear evidence of the accurate specifics of low-energy alternating electric fields. So that, this study will be conducted to measure of the electric field in emulated human body tissue.

Research that already exists today, wire mesh sensors or better known as WMS are used to detect the spread of bubble sizes in the fluid flow [10, 11, 12, 13]. The principle of this sensor is to obtain measurement data at each point of intersection wire. By providing an excitation voltage on one channel of the transmitter wire in turn. Moreover, the wire channel of the receiver will read in parallel. So that the bubble size distribution in the form of a two-dimensional 2D image. The disadvantage of this sensor is that when there is another external voltage source applied to the system, the signal readings on the receiver wire will be interrupted.

Therefore, this study will present a new method to get measurement data at each point of intersection wire if given external voltage source generated from capacitive electrode of ECCT. That is all wire channel act as receivers. This present study will conduct measurements of electric field intensity distribution accurately using wire mesh sensors. There will compare

between the characterization of wire mesh sensor 3×3 and 8×8 on air medium and phantom medium of emulated human body tissue. Phantom material is made with materials that have characterization resembles human body tissue. The experimental results will be reconstructed into a two-dimensional image of the electric field distribution on a cross-section. The image reconstruction results of the electric field distribution will be refined using bilinear interpolation to obtain a higher resolution.

2.0 METHODOLOGY

Wire Mesh Sensor for ECCT

The ECCT system consists of several capacitive electrodes and is connected to an AC voltage generator with a frequency 100 – 200 kHz via coaxial cable. The capacitive electrodes are attached to a particular human body and as two parallel plates with the principle of capacitors to disrupt the growth of cancer cells [6]. The ECCT system in this cylindrical body model consists of two capacitive electrodes which are placed at the top and bottom as shown in Figure 1.

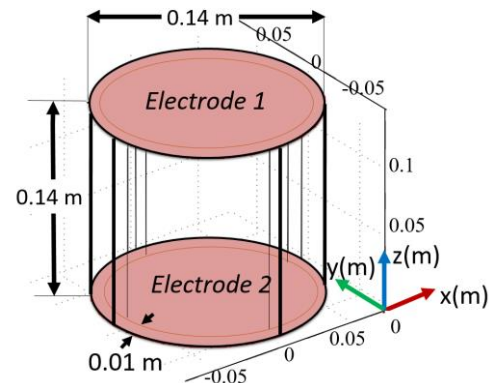


Figure 1 3D cylindrical body model with capacitive electrodes

Sensor Design

The conventional wire mesh sensor consists of two wire channels is transmitters (T_x) and receivers (R_x) arranged in parallel with 90° angles between the two wire channels. There is a distance between the two channels [13], described in Figure 2.

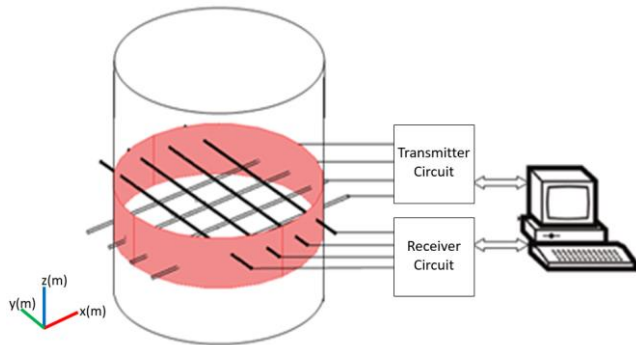


Figure 2 Schematic conventional wire mesh sensor to tomography image

The wire mesh sensor in this study only had channel receivers as shown in Figure 3. This wire mesh sensor had not channel transmitter because this sensor used to detect the electric field distribution value at each point of intersection wire generated voltage source from two electrode of ECCT placed at top and bottom tube. In this study using wire mesh sensor 8 × 8 because will get 64 points of voltage and electric field values, 64 points of this value are enough to get the distribution of electric field values. This study also uses wire mesh sensor 3 × 3 with 9 points of voltage and electric field values to compared with 64 points of distribution electric field from wire mesh sensor 8 × 8. Figure 3 shows the acquisition data for wire mesh sensor 3 × 3 and 8 × 8.

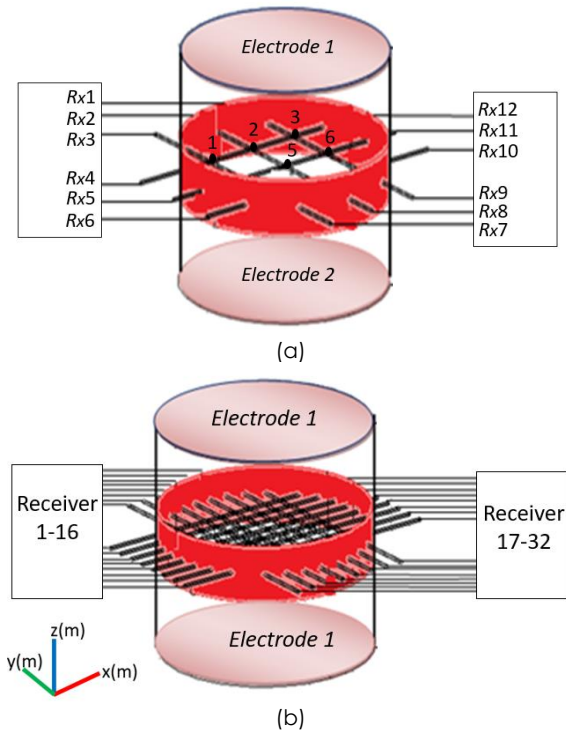


Figure 3 The acquisition data for wire mesh sensor: (a) 3 × 3, (b) 8 × 8

It can be seen in Figure 3 that the sensor all ends of the wire act as receivers. For wire mesh sensor 3 × 3 had nine voltage points of intersection wire that are searched by Laplace 3D using the amount of receiver of the measured voltage was 12. In this study, Laplace 3D finite difference was used to get the value of voltage and electric field at each point of intersection wire. 12 channel receiver in the wire mesh sensor 3 × 3 were used to detect the voltage values provided by the capacitive electrode of ECCT. The two electrode placed on the top and bottom of the tube and given voltage of 10 V at the top electrode and 0 V at the bottom electrode with a frequency of 100 kHz.

Laplace 3D finite difference can be modelled in Figure 4. To get the value of the voltage at each point of intersection wire can be calculated using Laplace 3D equation [14]. Points 1 and 2 are voltages measured from the receiver channel on the right and left sides of the tube or on the x axis. Points 3 and 4 are voltage measured from the receiver channel on the front and back sides of the tube or on the y axis. While points 5 and 6 are voltage source from two capacitive electrode located at the top and bottom of the vessel or on the z axis. So that the voltage value at the point of intersection wire can be obtained using Laplace 3D finite difference.

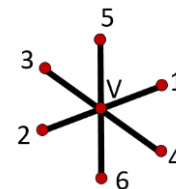


Figure 4 Laplace Model 3D finite difference

The voltage value at the point of V (centre) can be determined by first knowing the value of the point 1 (right), point 2 (left), point 3 (back), point 4 (front), point 5 (top) and point 6 (bottom). Furthermore, the six points are summed and subdivided 6. In mathematics can be written as follows [14]:

$$V = \frac{V(1)+V(2)+V(3)+V(4)+V(5)+V(6)}{6} \tag{1}$$

with:

- V = the voltage value at the midpoint
- V(1) = the voltage value at point 1 (+x axis)
- V(2) = the voltage value at point 2 (-x axis)
- V(3) = the voltage value at point 3 (+y axis)
- V(4) = the voltage value at point 4 (-y axis)
- V(5) = the voltage value at point 5 (+z axis)
- V(6) = the voltage value at point 6 (-z axis)

In order to get voltage value at intersection point 1 at wire mesh sensor 3×3 in Figure 2(a) with principle Laplace 3D can used :

$$V_1 = \frac{V_{Rx12} + V_{Rx4} + V_{Rx3} + V_{Rx7} + V_{top} + V_{bottom}}{6} \tag{2}$$

With the same way can determine the voltage value at the other point of intersection wire.

By using Laplace 3D equation then obtained nine values of the voltage at each point of intersection of wire to wire mesh sensor 3 × 3. Then the voltage value will be converted to the electric field value by the Equation [15]:

$$E = V/r \tag{3}$$

Where **E** is an electric field (V/m), **V** is voltage (V), and *r* is a distance of the point from a voltage source (m).

Shown in Figure 3(b), the principle of wire mesh sensor 8 × 8. The amount of voltage and electric field that resulted from wire mesh sensor depends on the topology of wire mesh sensor that used namely 3 × 3, 4 × 4, 8 × 8, and so on. In other words, the more the voltage value and the electric field it produces depends on the configuration of the wire mesh.

Image Reconstruction

Furthermore, image reconstruction will be conducted to obtain two-dimensional electric field distribution. The image reconstruction of the electric field distribution in wire mesh sensor using the principle of electrical capacitance tomography (ECT) [16]. The principle of ECT used two methods namely forward problem and inverse problem. In the forward problem of ECT, the capacitance data collected from the electrodes around the vessel outside the vessel wall. But in this study, in the forward problem, the electric field data collected from the channel receiver of wire. While the inverse problem of ECT is the image reconstruction of the capacitance measurement data. And the inverse problem in this study is the image reconstruction of the electric field measurement data.

In forward problem, we measure the voltage from the channel receiver of wire. And then the voltage is normalized.

$$V_n = \frac{V_p - V_a}{V_w - V_a} \tag{4}$$

Where V_n is normalized voltage, V_p is voltage in phantom medium, V_a is voltage in air medium, and V_w is voltage in water medium.

This forward problem uses a linearization technique called sensitivity model as follows [16]:

$$S_{0j} \cong V_{0j} \frac{E_{si}(x,y,z) \cdot E_{di}(x,y,z)}{V_{si}V_{di}} \tag{5}$$

Where $E_{si}(= -\nabla\phi)$ is the vector of the electric field distribution when the source electrode is active with the voltage V_{si} , and E_{di} is the vector of the electric field distribution when the active detector electrode is V_{di} voltage. V_{0j} is the voxel volume. The linearization of the sensitivity is [16]:

$$C = GS \tag{6}$$

Where C is represents V_n and G is represents electric field

as a function of permittivity. Since the inverse S does not exist then the linear backpropagation technique (LBP) is used [16]:

$$G = S^T V_n \tag{7}$$

In order to get the image reconstruction of electric field distribution with higher resolution, bilinear interpolation was used. Study on image reconstruction based on wire mesh sensor using five interpolation algorithm. The object created image is a mixture of oil and water. The five algorithms performed, the best algorithm is bilinear interpolation algorithm and inverse distance square weighting algorithm [17]. The equation on bilinear interpolation algorithm (see Figure 5) can be calculated as follows [15]:

$$O = K * (1 - S) * (1 - T) + L * T * (1 - S) + M * S * (1 - T) + N * S * T \tag{8}$$

With O is point to be found. K, L, M, N are measurement point. S, T are distance.

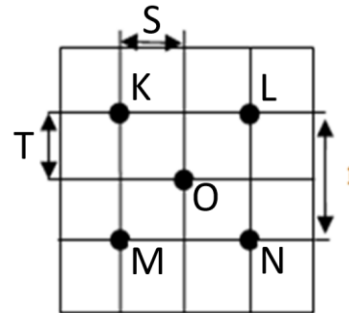


Figure 5 Bilinear interpolation method

Phantom Condition

The fabricated phantom as an emulated human body tissue was made from 250 mL of H₂O, 150 mL of Silicon rubber, 150 mL of Glycerin, 27.5 g of Agar, and 3 g of NaCl. In order to create a phantom is to first weigh all the ingredients according to size. Then mix all the ingredients in a container, and heat over the heat until mixed evenly. Then cool the ingredients and insert them in the mold.

3.0 RESULTS AND DISCUSSION

The measurement of the electric field in emulated human body tissue using wire mesh sensor successfully done. Wire mesh sensors 3 × 3 and 8 × 8 have been successfully fabricated and analysed for this study (see Figure 6).

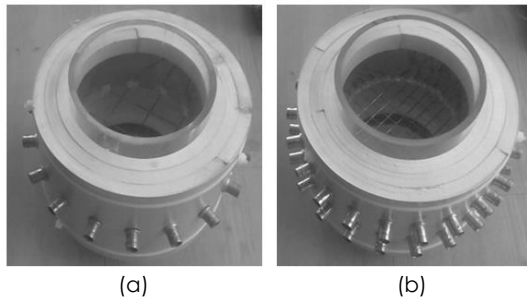


Figure 6 (a) Wire mesh sensor 3×3 , (b) Wire mesh sensor 8×8

The wire material is copper with a diameter of 1 mm. The material of the tube is acrylic with a diameter of 14 cm and a height of 14 cm. Wire mesh placed in the centre of the tube. The mesh distance is 3 cm for WMS 3×3 and 1 cm for WMS 8×8 .

In this study, the electric field distribution using both wire meshes were conducted with and without phantom as an emulated human body tissue. The fabricated phantom characteristics that resemble human body tissue are presented in Figure 7.

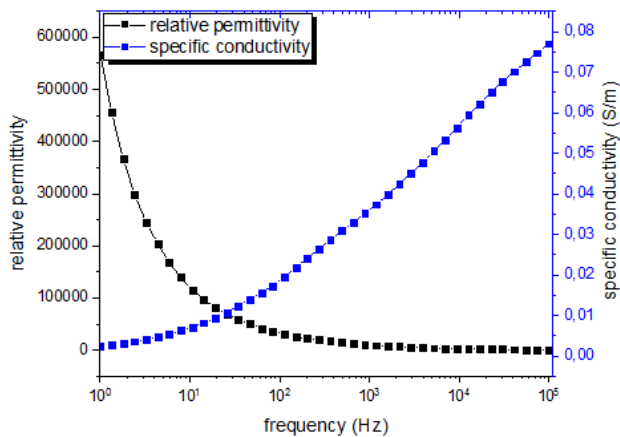


Figure 7 Frequency dependence of the relative permittivity and specific conductivity of phantom material

It can be analyzed from Figure 7 that the relative permittivity value in the emulated human body tissue at low frequency has high value, while at high frequency has low value. The conductivity value of phantom material at low frequency has a low value, while at high frequency has a high value. The fact is in accordance with Damijan [18] that the higher frequency made the relative permittivity of human body tissue decreased. Conversely, the higher frequency made the conductivity of the human body tissue increases.

The electric field distribution simulation and experiments have been done using an external voltage source from capacitive electrode ECCT of 10 V placed on a top tube, and 0 V placed on a bottom tube (see Figure 1).

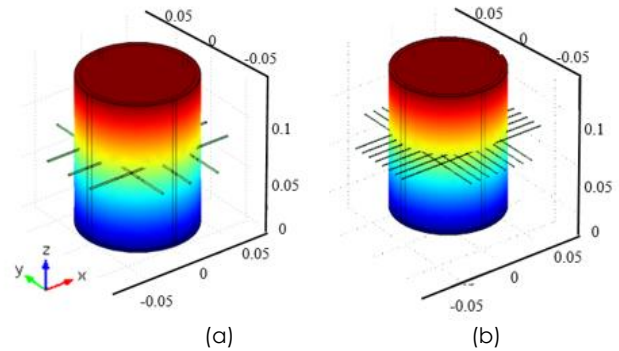


Figure 8 Voltage distribution of wire mesh sensor: (a) 3×3 , (b) 8×8

The result of simulation is summarized in Figure 8 and Figure 9. In Figure 8(a) shows the voltage distribution using wire mesh sensor 3×3 and Figure 8(b) shows the voltage distribution using wire mesh sensor 8×8 . In Figure 9(a) shows direction of electric field due to external voltage source at wire mesh sensor 3×3 and Figure 9(b) shows direction of electric field due to external voltage source at wire mesh sensor 8×8 .

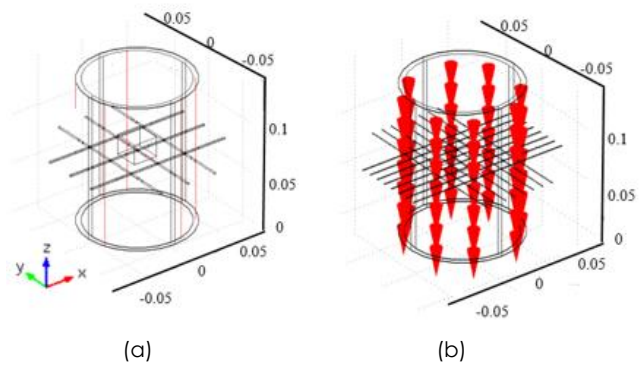


Figure 9 Direction of electric field due to external voltage source from two capacitive electrode of ECCT at wire mesh sensor: (a) 3×3 , (b) 8×8

The results of experiments are summarized in Figure 10 and Figure 11. In Figure 10(a) shows the electric field distribution using wire mesh sensor 3×3 for the air medium, while in Figure 10(b) shows the electric field distribution using phantom-treated wire mesh sensor 3×3 . This electric field distribution pattern is obtained using Laplace 3D equations and the voltage conversion formula to the electric field, as in Equations 1 and 3. Figure 11(a) shows the electric field distribution using wire mesh sensor 8×8 for the air medium, while in Figure 11(b) shows the electric field distribution using phantom-treated wire mesh sensor 8×8 . This electric field distribution pattern is obtained using Laplace 3D equations and the voltage conversion formula to the electric field, as in Equations 1 and 3.

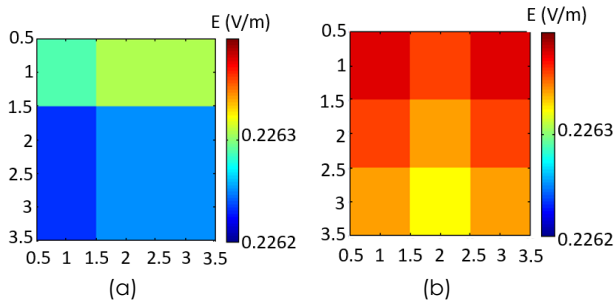


Figure 10 (a) Electric field distribution (V/m) of WMS 3 × 3 in the air, (b) Electric field distribution (V/m) of WMS 3 × 3 in phantom

Based on the electric field distribution pattern on WMS 3 × 3 (Figure 10) and WMS 8 × 8 (Figure 11) can be distinguished between air medium and phantom. For air medium there is the blue colour, it means a lower electric field value. For the medium phantom, there is a red colour which means the value of the electric field is high.

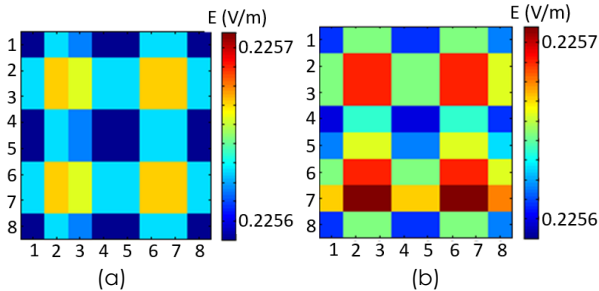


Figure 11 (a) Electric field distribution (V/m) of WMS 8 × 8 in the air, (b) Electric field distribution (V/m) of WMS 8 × 8 in phantom

The results are not yet compatible with Andiani [19], and Markus [20] where their research yields the reverse that the value of the electric field in the air is higher than the value of the electric field in human body tissue. For that reason, it is necessary to reconstruction image of electric field distribution using inverse principle linear back propagation refer to (7).

The results of reconstruction image electric field distribution on WMS 3 × 3 and WMS 8 × 8 in phantom are presented in Figure 11.

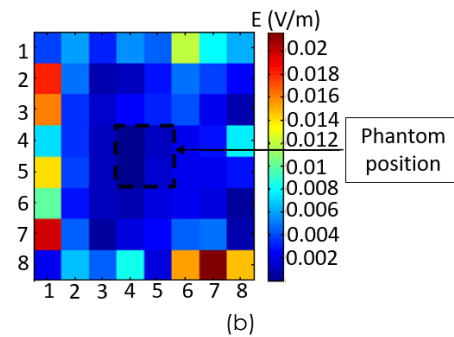
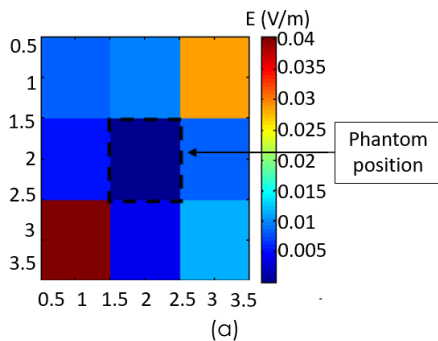


Figure 12 Reconstruction image of electric field distribution (V/m) in: (a) Wire Mesh Sensor 3 × 3 and (b) Wire Mesh Sensor 8 × 8

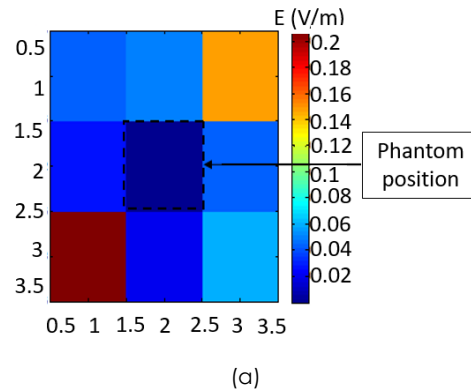
Based on the image reconstruction of the electric field distribution in Figure 12, there is a decrease of the electric field value at the existing point of its phantom compared to the point that there is no phantom (air medium). The relative permittivity value of phantom at 100 kHz is 653.16 (Measured using Electrical Impedance Spectroscopy). Meanwhile, the relative permittivity value of air is 1.

This result is in accordance with Gauss theory that the electric field value is inversely proportional to the permittivity value. The greater permittivity can make the value of the electric field to be smaller. This result also corresponds to Andiani [19] that the electric field in the air medium is higher than the electric field in the human body tissue. Andiani reported that the highest electric field value was 151.06 V/m in air medium and 0.46 V/m in anatomy medium. The law of Gauss in difference is [21].

$$\nabla \cdot \vec{E} = \frac{\rho}{\epsilon_0} \tag{8}$$

The electric field value is inversely proportional to the permittivity value.

The results of image electric field distribution reconstruction can be compared with the simulation results of electric field distribution. For the simulation results of the electric field distribution can be seen in the Figure 13.



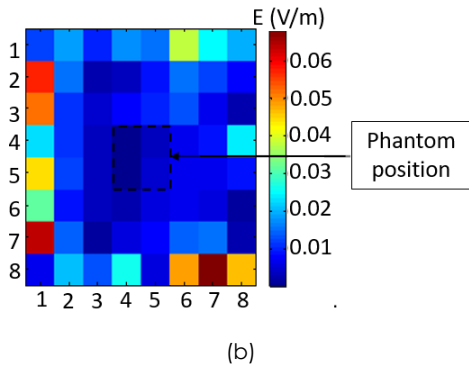


Figure 13 Simulation of electric field distribution (V/m) in: (a) wire mesh sensor 3x3 and (b) wire mesh sensor 8x8

The average value of the electric field distribution of the simulation results in wire mesh sensor 3 x 3 is 0,066857 V/m, whereas the average value of the electric field distribution of the reconstruction in wire mesh sensor 3x3 is 0,012978 V/m. There is difference of average value of electric field distribution equal to 80.59%.

The average value of the electric field distribution of the simulation results in wire mesh sensor 8 x 8 is 0,015521 V/m, whereas the average value of the electric field distribution of the reconstruction in wire mesh sensor 8 x 8 is 0,00488 V/m. There is difference of average value of electric field distribution equal to 68.56%.

The image reconstruction results in the wire mesh sensor 3 x 3 (Figure 12(a)) can be refined into WMS 5 x 5 using bilinear interpolation and generate a comparison of the electric field value between the existing wire intersection point of its phantom and no phantom (air medium) of 61.8%. Meanwhile, the image reconstruction results in the wire mesh sensor 8 x 8 (Figure 12(b)) can be refined into WMS 15x15 using bilinear interpolation and generate the comparison of the electric field value between the existing wire intersection point of its phantom and no phantom (air medium) of 82.42%. Based on Figure 12, can be seen that wire mesh sensor 8 x 8 have a resolution of electric field distribution is higher than wire mesh sensor 3 x 3. So wire mesh sensor 8 x 8 better than wire mesh sensor 3 x 3.

The Bilinear interpolation refer to (8) was used to get the image reconstruction of electric field distribution with higher resolution.

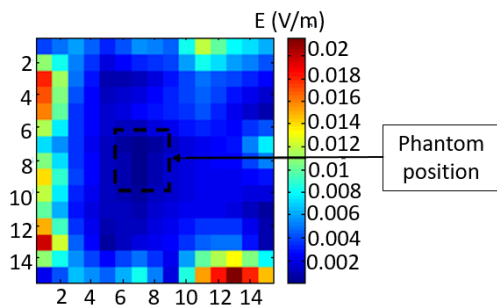


Figure 14 WMS 8 x 8 electric field distribution (V/m) pattern after interpolation

Based on the pattern of electric field distribution with higher resolution (Figure 14), the average value of the electric field in the phantom that resembles human body tissue is 8.0×10^{-4} V/m while the mean value of the electric field in the air medium that has no phantom is 4.6×10^{-3} V / m. There was a decrease of electric field value between medium air and phantom medium equal to 82.42%.

Phantom position in tube with wire mesh sensor 3 x 3 can be seen in Figure 15. This inclusion shaped phantom is placed in the middle of wire mesh sensor.

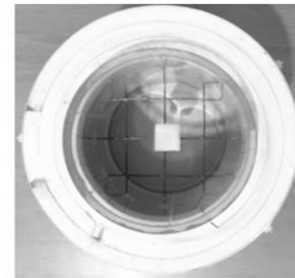


Figure 15 Phantom position in WMS 3 x 3

4.0 CONCLUSION

It can be concluded that wire mesh sensors can be used to detect electric fields on human body tissues when given an outer voltage source from two capacitive electrode of ECCT. Moreover, wire mesh sensors also produce electric field distribution tomography with higher resolution.

There is a decrease in the value of the electric field between the phantom that resembles the human body tissue ($\epsilon_r = 653.16$) with the air medium ($\epsilon_r = 1$) of 82.42% for WMS 8 x 8 and 61.8% for WMS 3 x 3. It is in accordance with Gauss's Law that the greater permittivity of material makes the smaller value of the electric field. Moreover, wire mesh sensor 8 x 8 is a better resolution than wire mesh sensor 3 x 3

Acknowledgement

This work was supported in part by the C-Tech Lab Edwar Technology, in part by Indonesian Institute of Science, LIPI physics, Indonesia and in part by Directorate General of Higher Education, DIKTI, Indonesia.

References

- [1] E. D. Kirson, Z. Gurvich, R. Schneiderman, E. Dekel, A. Itzhaki, Y. Wasserman, R. Schatzberger, and Y. Palti. 2004. Disruption of Cancer Cell Replication by Alternating Electric Fields. *Cancer Res.* 64(9): 3288-95.
- [2] E. D. Kirson, V. Dbalý, F. Tovaryš, J. Vymazal, J. F. Soustiel, A. Itzhaki, D. Mordechovich, S. Steinberg-Shapira, Z. Gurvich, R. Schneiderman, Y. Wasserman, M. Salzberg, B. Ryffel, D. Goldsher, E. Dekel, and Y. Palti. 2007. Alternating Electric fields Arrest Cell Proliferation in Animal Tumor Models and

- Human Brain Tumors. *Proc. Natl. Acad. Sci.* 104(24): 10152-10157.
- [3] R. Nuccitelli, U. Pliquett, X. Chen, W. Ford, R. James Swanson, S. J. Beebe, J. F. Kolb, and K. H. Schoenbach. 2006. Nanosecond Pulsed Electric Fields Cause Melanomas to Self-destruct. *Biochem. Biophys. Res. Commun.* 343(2): 351-360.
- [4] L. Carr, S. M. Bardet, R. C. Burke, D. Arnaud-Cormos, P. Leveque, and R. P. O'Connor. 2017. Calcium-independent Disruption of Microtubule Dynamics by Nanosecond Pulsed Electric Fields in U87 Human Glioblastoma Cells. *Sci. Rep.* 7: (7252): 1-12.
- [5] S. A. Mujib, F. Alamsyah, and W. P. Taruno. 2017. Cell Death and Induced p53 Expression in Oral Cancer, HeLa, and Bone Marrow Mesenchyme Cells under the Exposure to Noncontact Electric Fields. *Integr. Med. Int.* 4(3-4): 161-170.
- [6] W. P. Taruno. 2017. Kapasitif Elektro Terapi (Alat Terapi Penyakit Kanker). 2013/03941.
- [7] F. Alamsyah, I. N. Ajrina, F. N. A. Dewi, D. Iskandriati, S. A. Prabandari, and W. P. Taruno. 2017. Antiproliferative Effect of Electric Fields on Breast Tumor Cells In Vitro and In Vivo. *Indones. J. Cancer Chemoprevention.* 6(3): 71.
- [8] M. Giladi, U. Weinberg, R. S. Schneiderman, Y. Porat, M. Munster, T. Voloshin, R. Blatt, S. Cahal, A. Itzhaki, A. Onn, E. D. Kirson, and Y. Palti. 2014. Alternating Electric Fields (Tumor-Treating Fields Therapy) Can Improve Chemotherapy Treatment Efficacy in Non-Small Cell Lung Cancer Both In Vitro and In Vivo. *Semin. Oncol.* 41: S35-S41.
- [9] F. Topfer and J. Oberhammer. 2015. Millimeter-wave Tissue Diagnosis: The Most Promising Fields for Medical Applications. *IEEE Microw. Mag.* 16(4): 97-113.
- [10] H. Prasser, D. Scholz, and C. Zippe. 2001. Bubble Size Measurement Using Wire-mesh Sensors. *Flow Meas. Instrum. Elsevier.* 12: 299-312.
- [11] M. J. Da Silva, E. Schleicher, and U. Hampel. 2007. Capacitance Wire-mesh Sensor for Fast Measurement of Phase Fraction Distributions. *Meas. Sci. Technol.* 18(7): 2245-2251.
- [12] B. J. Azzopardi, L. a. Abdulkareem, D. Zhao, S. Thiele, M. J. da Silva, M. Beyer, and a. Hunt. 2010. Comparison between Electrical Capacitance Tomography and Wire Mesh Sensor Output for Air/Silicone Oil Flow in a Vertical Pipe. *Ind. Eng. Chem. Res.* 49(18): 8805-8811.
- [13] H. F. Velasco Peña and O. M. H. Rodrigue. 2015. Applications of Wire-mesh Sensors in Multiphase Flows. *Flow Meas. Instrum.* 45: 255-273.
- [14] D. W. Harder. 2012. *Laplace's Equation in 2 and 3 Dimensions*. Waterloo, Ontario, Canada.
- [15] D. H. Staelin. 2011. *Electromagnetics and Applications*. Dep. Electr. Eng. Comput. Sci. Massachusetts Inst. Technol. Cambridge, MA. 1-442.
- [16] W. Warsito, Q. Marashdeh, and L. S. Fan. 2007. Electrical Capacitance Volume Tomography. *IEEE Sens. J.* 7(4): 525-535.
- [17] P. Chen, Y. Ji, and N. Jin. 2012. *Study on Image Reconstruction Algorithms for Wire Mesh Tomography System*. Springer, Berlin, Heidelberg. 133-138.
- [18] D. Miklavčič, N. Pavšelj, and F. X. Hart. 2006. *Electric Properties of Tissues*. Wiley Encycl. Biomed. Eng. 1-12.
- [19] L. Andiani, Endarko, M. Al Huda, and W. P. Taruno. 2017. A Novel Method for Analyzing Electric Field Distribution of Electro Capacitive Cancer Treatment (ECCT) Using Wire Mesh Electrodes: A Case Study of Brain Cancer Therapy. *EuroMediterranean Biomed. J.* 12(38): 178-183.
- [20] M. Handriyanto. 2006. Electro-Capacitive Cancer Treatment (ECCT) Effectiveness for Brain Cancer. Univ. Indones.
- [21] LEA and BURKE. 2013. Electric Fields in Dielectrics. *Phys. 360 - Electr. Magn.* 1: 1-10.